Sensitivity Of Surface Acoustic Wave Sensors Based $LiNbO_3$ 128 ° Y-X and AT-quartz to PM10 and PM2.5.

Dbibih Fatima-Ezzahraa, Virginie Blondeau-Pâtissier, Lyes Djoumi, Valérie Souman ,meddy vanotti

Introduction

Particulate matter (PM) was estimated to cause around 7 million premature deaths worldwide per year according to World Health organization [1]. These particles can cause diseases leading to premature death [2]. Over the last decade, the monitoring of PM became an important issue on a worldwide scale.The miniaturization of the existing bulky systems has also become necessary to reduce their cost. To address this need, a new miniaturized system for PM monitoring was previously developed in our team [3].It takes advantage of both a 3 Lpm cascade impactor and surface acoustic waves (SAW) sensors to respectively separate and measure particles. The present study aims to compare the sensitivity of two SAW devices. The first exploits Love waves on an ATcut Quartz substrate and the second is based on Rayleigh waves from a $LiNbO_3$ Y-X 128° substrates. The latter presents a high electromechanical coupling factor that could be exploited for the self-cleaning of the device after the measurement. This could allow overcoming the fouling issue faced with impactors that wouldn't be solved with quartz based sensors which suffer from an insufficient electromechanical coupling.

Method

In this study we used a dedicated 3 Lpm cascade impactor equipped with SAW delay lines as collecting plate. The Rayleigh wave sensor and the Love wave sensor were designed and fabricated respectively on $LiNbO_3$ Y-X 128° cut and AT-Quartz cut substrates using a conventional photolithography process. The interdigital transducers (IDT) consist of double finger pairs made of 200 nm thick aluminum with a periodicity p=10 µm and a wavelength λ=40 µm. Hence, the working frequency is 125 MHz for the Love mode and 98 MHz for the Rayleigh mode.. The propagation of Love wave needs a guiding layer. For that purpose, a silica layer was deposited using sputtering technique with shear velocity lower than the piezoelectric substrates. The region between the two IDTs constitutes the sensing area.

Preliminary tests have been performed using candle smoke. As the obtained PM concentrations were unstable and difficult to reproduce, we have developed an experimental set-up bench consisting of a $1m^3$ chamber, a particle's generator AGK 2000 and an optical system FIDAS® 100. Thus, sodium chloride (NaCl) was used to produce PM2.5 while PM10 were generated from silicon carbide (SiC) in the 0 to 200 $\mu g/m^3$ concentration range.When the particles impact on the sensor surface, the velocity of the acoustic waves decreases due to the sensors' high gravimetric sensitivity. Accordingly, the wave phase velocity shift is measured by monitoring the phase at constant frequency with an open loop interrogation [4]. It's then correlated to the particles concentration.

Results and Conclusions

Figure 1 and 2 shows plots of phase derivative dϕ/dt of sensors-based AT-Quartz (black) and $LiNbO_3$ (red) with the concentration of PM10 and PM2.5 respectively measured with the optical system FIDAS®. As expected, the sensitivity of the Rayleigh wave sensor based on LiNbO3 is lower than the Love wave sensor based on quartz for both PM10 and PM2.5. The sensor's sensitivity is estimated by applying a linear fit of the plotted data. The sensitivity of sensors based on quartz is 3.10-4 °/s.µg/m3 for PM 2.5 and 5.10-5 °/s.µg/m3for PM10. For sensors based on LiNbO3, the sensitivity is 1.10-4 °/s.µg/m3 for PM2.5 and 1.10-5 °/s.µg/m3 for PM10. The feature that the sensors' response is greater with PM2.5 than with PM10 can be explained by the fact that most adhesion forces are linearly dependent on particle diameter [5] which is often described as the rebound effect. As a result, the smaller particles settle more on the surface of the sensor resulting in a more significant slowdown of the wave. To ensure that each stage is measuring the targeted size range, we took images of the sensors surface at the end of the experiment using a microscope. Figures 3,4 show the surface of the PM2.5 stage and figures 5,6 the one of the PM10 stage. One can observe that, as expected, the PM2.5 contain more particles than the PM10 and that the particle sizes correspond well to the ranges [0.3 µm, 2.5 µm] and [2.5 µm, 10 µm]. It has therefore been shown that LiNbO3 sensors, although less sensitive, can also be used for fine particles detection. They still need work to improve their performance and limit the rebound effect, but they remain very promising for the development of self-cleaning systems.

References

[1] « Air pollution ». https://www.who.int/news-room/fact-sheets/detail/ambient-(outdoor)-air-quality-and-health.

[2] H. Lin *et al.*, « Particle size and chemical constituents of ambient particulate pollution associated with cardiovascular mortality in Guangzhou, China », *Environmental Pollution*, vol. 208, p. 758‑766, janv. 2016.
[3] L. Djoumi, M. Vanotti, et V. Blondeau-Patissier, « Real Time Cascade Impactor Based On Surface Acoustic Wave Delay Lines for PM10 and PM2.5 Mass Concentration Measurement », *Sensors (Basel)*, vol. 18, nº 1, janv. 2018.
[4] D. Rabus, J. Friedt, S. Ballandras, G. Martin, E. Carry, et V. Blondeau-Patissier, « High-sensitivity open-loop electronics for gravimetric acoustic-wave-based sensors », *IEEE Transactions on Ultrasonics, Ferroelectrics, and Frequency Control*, vol. 60, nº 6, p. 1219‑1226, juin 2013.
[5] P. Kulkarni, P. A. Baron, et K. Willeke, « Introduction to Aerosol Characterization », in *Aerosol Measurement*, John Wiley & Sons, Ltd, 2011, p. 1‑13.

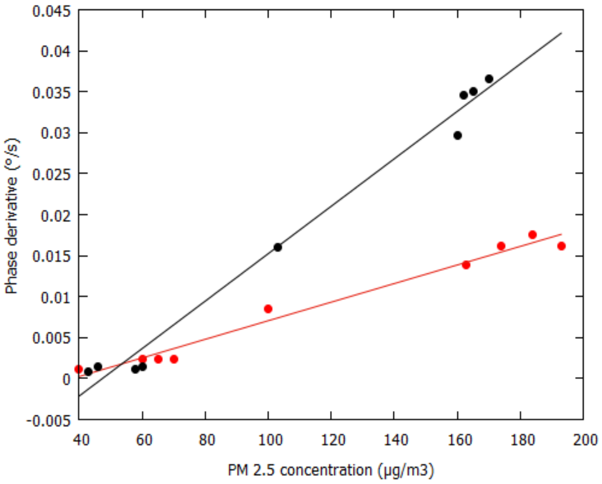

Figure 1 : Phase derivative of SAW sensors based $LiNbO_3$ Y-X 128 ° (red) and AT-Quartz (black) as a function of PM 2.5 concentration.

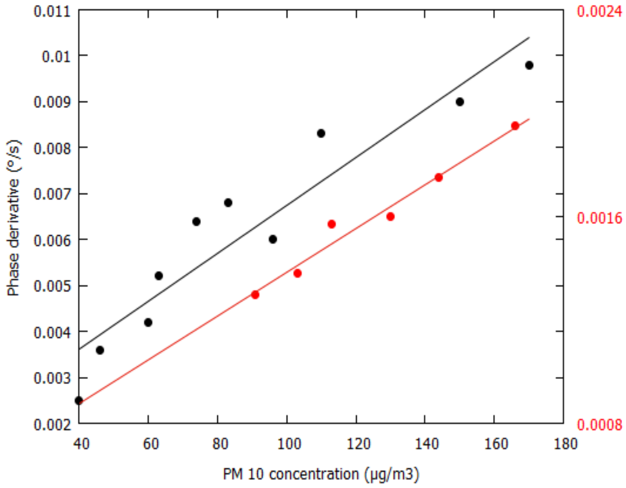

Figure 2 : Phase derivative of SAW sensors based $LiNbO_3$ Y-X 128 ° (red) and AT-Quartz (black) as a function of PM 10 concentration.

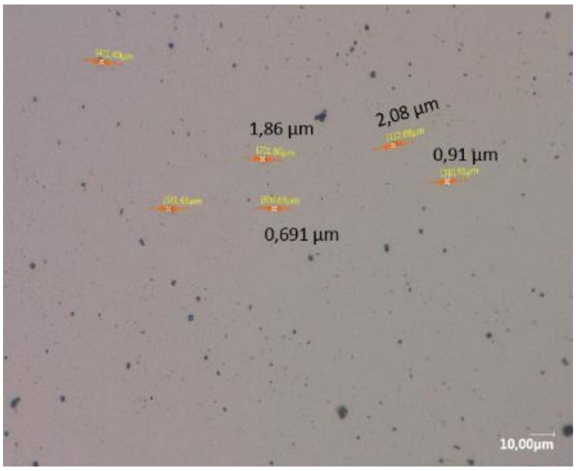

Figure 3: Image of the $LiNbO_3$ Y-X 128 ° sensor's surface after exposition to PM 2.5, zoom x1500.

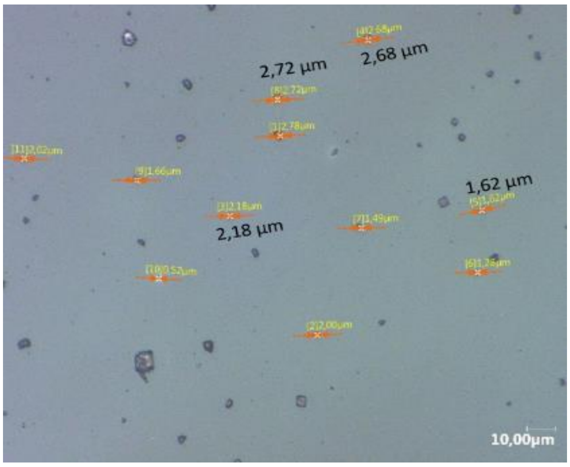

Figure 4: Image of the AT-quartz sensor's surface after exposition to PM 2.5, zoom x1500.

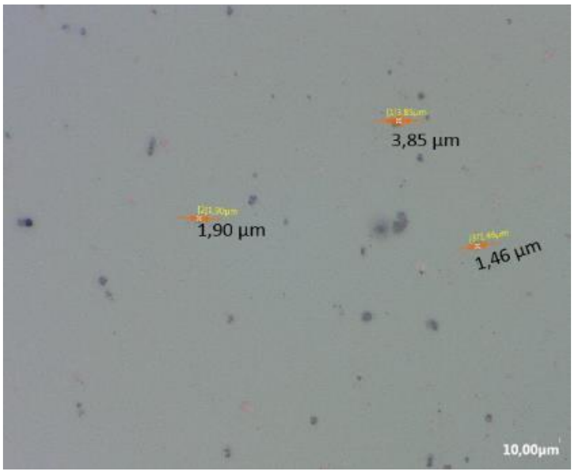

Figure 5: Image of the $LiNbO_3$ Y-X 128 ° sensor's surface after exposition to PM 10, zoom x1500.

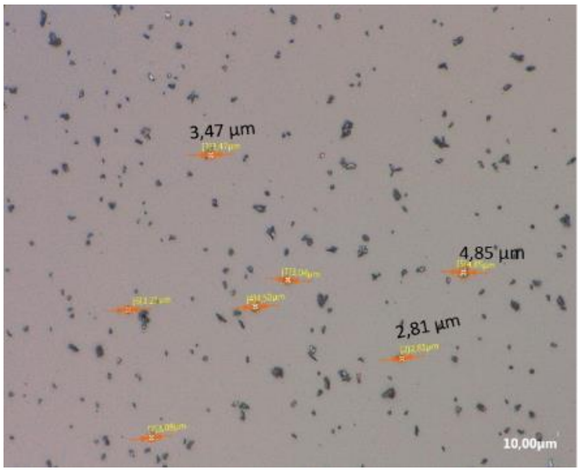

Figure 6: Image of the AT-quartz sensor's surface after exposition to PM 10, zoom x1500.